Geochemical Journal, Vol. 41, pp. 165 to 172, 2007

An attempt to determine the age of geological fractures by applying Rb–Sr mineral isochron dating to fracture-filling minerals

MARI T. ASAHARA and TSUYOSHI TANAKA*

Department of Earth and Planetary Sciences, Graduate School of Environmental Studies, Nagoya University, Chikusa, Nagoya 464-8602, Japan

(*Received March 1, 2006; Accepted January 30, 2007*)

Geological fractures commonly contain the minerals calcite and zeolite, which have crystallized in the fracture after its formation. The minimum age of formation of the fracture can be estimated from the age of the fracture-filling minerals. We tried to determine the age of fracturing by applying the Rb–Sr mineral isochron method to the fracture-filling paragenetic calcite and zeolite samples from fractures in the Kurihashi granodiorite and a skarn in the Kamaishi mine in northeastern Japan.

The age of crystallization of fracture-filling minerals was estimated to be in the range 74 to 58 Ma in the Kurihashi granodiorite. The main causes of fracturing were considered to be igneous activities and the cooling of magma. We could not determine ages for some of the fractures we investigated, probably because of the subsequent low-temperature alteration after fracturing, or because of host wall rock contamination of the fracture-filling mineral samples.

The ages determined for fractures in the skarn pre-dated the skarnization process. It is possible that these fractures formed before the skarnization. However, selective leaching of rubidium during skarnization reduces the Rb/Sr ratio. Therefore, skarnization can have the effect of producing erroneously old Rb–Sr ages.

From the initial $^{87}Sr/^{86}Sr$ ratios, we determined changes in the strontium isotopic ratio in the local groundwater from the Late Cretaceous through the Paleocene, noting a significant increase at 62 Ma.

Keywords: geochronology, Rb-Sr dating, fracture-filling mineral ishchron, Kamaishi mine, application of Rb-Sr isochron method

INTRODUCTION

The age of geological fractures, including faults, is an important factor when we consider the stability of the geological environment, such as the period between major earthquakes. The methods used for dating fractures are commonly based on determining the age of fracture-filling minerals and include the electron spin resonance (ESR) method for fracture quartz and feldspars (Ikeya *et al*., 1982), the fission track (FT) method for fracture epidote (Bar *et al*., 1974), the K–Ar dating method for fault gouge material or fracture clay minerals (Shibata *et al*., 1989; Cathelineau *et al*., 2004), and the Rb–Sr dating method for clay minerals (Rousset and Clauer, 2003). However, each of these methods has flaws.

In the ESR method, the defect lattice caused by radiation damage is measured by examining unpaired electrons. The defect lattice must remain stable after fracturing, as secondary defects skew the dating results. It is also necessary for the formation of defect lattice to be undersaturated.

In the FT method, the closure temperature of commonly used minerals is very low (110°C for apatite and 200°C for zircon) and the FTs will be destroyed by subsequent thermal metamorphism that exceeds these temperatures. The Subcommission on Geochronology recommended that the FT ages should be obtained by the zeta method (Hurford, 1990). Ages obtained by the zeta method are comparable to those obtained by other radiometric methods (e.g., K–Ar age and Ar–Ar age) in that they are relative ages, determined by comparison to known standards.

The K–Ar method of dating fractures is dependent on the presence of gouge in the fractures, which is not always the case. This method also requires the presence of K-rich authigenic minerals in the fracture.

Rousset and Clauer (2003) calculated Rb–Sr "isochron" ages by only two fractions (HCl-leachate and residue) clay components, although these ages are in agreement with K–Ar ages. In this study, we used the Rb–Sr mineral isochron method to fracture-filling paragenetic calcite and zeolite to determine the ages of fractures. Calcite and zeolite are common fracture-filling minerals. These minerals take up rubidium and strontium from groundwater at different Rb/Sr ratios giving different $^{87}Sr/^{86}Sr$ ratios at the present time. The minimum age of for-

*Corresponding author (e-mail: tanaka@eps.nagoya-u.ac.jp)

Table 1. Sample descriptions

Sample	Host wall rock	Descriptions
#20	Kurihashi granodiorite	Collected at 250 m level gallery. The host rock around this vein turns red. Epidote (1 cm) and mixture of calcite and zeolite (1 cm) are crystallized on the rock, in this order.
1		The mixture of calcite and zeolite.
2		Epidote rich section.
#133	Kurihashi granodiorite	Collected at 550 m level gallery. Calcite blocks are found in zeolite. Zeolite also contains chlorite in part.
all		All mineral fragments of fracture.
1		Only calcite rich section.
1~5		Calcite rich section scraped off vertically to the cleavage face in every 5 mm. Number shows the order from the wall rock.
6		Chlorite-containing section.
2		Zeolite-rich section.
#153	Kurihashi granodiorite	Collected at 550 m level gallery. Zeolite and calcite are crystallized on the host rock, in this order. Boundaries between minerals are unclear.
1		Pink-colored section.
2		Sheet structured section of calcite and zeolite.
all		All mineral fragments of sheet structure section.
1~2		Sheet structured section scraped off vertically to the cleavage face in every 5 mm. Number shows the order from farther to nearer part on the rock.
CVS	Skarn	Collected at 550 m level gallery. The width of this fracture is 2 cm. Small pyrite and chlorite were crystallized on the surface of calcite.
all		All mineral fragments of vein.
1~3		Only calcite and zeolite scraped off vertically to the cleavage face in every 5 mm. Number shows the order from the wall rock.
4		Chlorite-containing section.

Fig. 1. Location and geological map of the Kamaishi mine showing sampling points.

mation of the fracture can be estimated from the age of crystallization of the fracture-filling minerals, because the minerals post-date fracture formation.

SAMPLES

Samples were collected from the 250 m and the 550 m galleries in the Kamaishi mine, Iwate prefecture, northeastern Japan (Fig. 1). This area is mainly underlain by Kurihashi granodiorite, Ganidake complex, skarn and Permian slate. The skarn is considered to have formed by the intrusion of the Ganidake complex into the Carboniferous limestone. The subsequent intrusion of the Kurihashi granodiorite had no effect on the surrounding rocks (Hamabe and Yano, 1976). The Rb–Sr mineral isochron age of the Kurihashi granodiorite has been determined to be 120 ± 14 Ma (Takagi *et al*., 2001a).

Fracture-filling mineral samples were collected from fractures in the Kurihashi granodiorite (sample locations #20, #133 and #153) and in the skarn (sample location CVS) as shown in Fig. 1. At location #20, high temperature alteration zone (mainly epidote) and low temperature alteration zone (mainly calcite) are clearly evident on red-colored altered host wall rock. Only the sample location #20 contains epidote. Samples from locations #133 and the #153 include calcium-rich fracture-filling minerals (mainly calcite, laumontite and prehnite) on red-colored altered host wall rock. At the location #133, calcite was found in zeolite. At the location #153, however, very thin banded calcite and zeolite were crystallized.

According to Amano *et al*. (1999) and Yoshida *et al*. (2000), at the fracture with red-colored alteration haloes at such locations as #20, #133 and #153, fracture filling minerals were changing from the high-temperature type

(mainly composed of epidote, prehnite and laumontite; temperature range 400 to 200°C) to the low-temperature type (mainly composed of stilbite, chlorite and calcite; temperature lower than 200°C). Under microscopic observation, the low-temperature type minerals occur in bands a few millimeters in width parallel to with the fracture. Narrow calcite vein grades into laumontite in some areas. It is considered that the low-temperature type minerals examined here were crystallized at the same time.

The CVS sample was collected from a vein of greenish skarn, which contained minor pyrite crystals on the surface. All samples were collected together with their host wall rocks. According to their petrographic and X-ray diffraction (XRD) studies, calcite, zeolite (stilbite and laumontite) and gypsum in these fracture-filling mineral samples had crystallized from groundwater at the same time (Amano *et al*., 1999; Yoshida *et al*., 2000).

The collected samples were ultrasonically cleaned in distilled, de-ionized water and dried at 60°C. Each of the original four samples was divided based on visible differences (#20-1, #20-2, #133-all, #133-1, #133-2, #153-1, #153-2 and CVS). Some of the sub-samples were further subdivided and treated as follows: (1) Host wall rock was removed and the remainder was powdered in a stainless steel mortar. This powder was treated as a single sample which represents whole fracture (samples #20-1, #20-2, #133-all, #133-2, #153-1, #153-2-all and CVS-all). (2) Fracture-filling mineral was scraped off vertically to the cleavage face in every 5 mm and powdered. These samples were used to determine the relationship between distance from the host wall rock and fracture-filling mineral age (samples #133-1 series, #153-2 series and CVS-1 to 4). Sample descriptions are shown in Table 1.

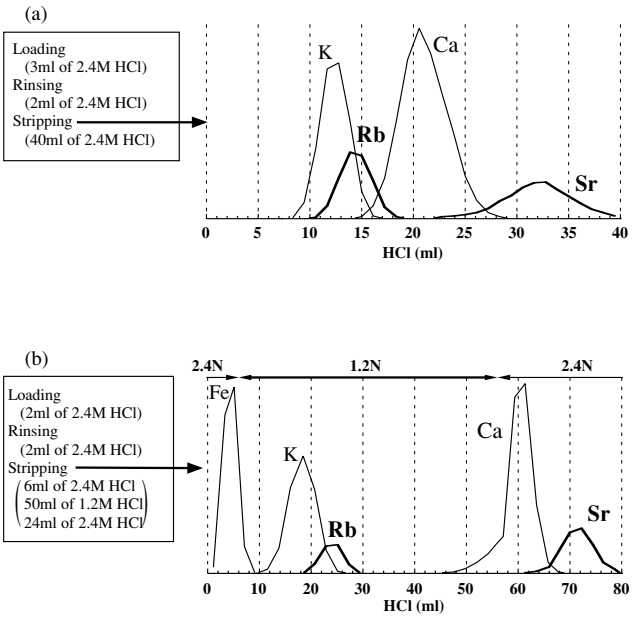

Fig. 2. Results of the column separation. (a) Conventional method used 2.4 M hydrochloric acid as an eluent. (b) Method used in this study combining 1.2 M and 2.4 M hydrochloric acid as eluents to improve separation of rubidium from potassium and calcium.

Analytical Methods

The powdered samples (*ca*. 0.2 g) were placed in PE centrifuge tubes and 5 ml of 50% acetic acid was added to dissolve the contained calcite. We did not use hydrochloric acid for leaching calcite because of the presence of laumontite, a zeolite that reacts with hydrochloric acid to produce gelatinous material (Murata, 1943). The leachate was poured into a PTFE beaker and the residue was cleaned with distilled water twice and cleaning water was added into the same PTFE beaker before drying. The leachate was dissolved in hydrochloric acid and dried again to convert the chloride forms for a subsequent procedure. The residue in the PE tube was zeolite. The residual zeolite was dried and analyzed using an XRD (RIGAKU RAD-C2, with a copper target and nickel filter, operating at 40 kV and 20 mA) to check that no calcite remained. Both zeolite and mixed fracture-filling minerals (*ca*. 0.2 g) were digested with 5 ml of 50% hydrofluoric acid and 2 ml of concentrated perchloric acid and dried.

All digested samples were dissolved in 2.4 M hydrochloric acid, split into two aliquots. ^{87}Rb- and ^{84}Sr-enriched spikes were added to one aliquot for isotope dilution analyses of rubidium and strontium. The other aliquot was used for strontium isotopic analyses. After drying, they were dissolved in 2 ml of 2.4 M hydrochloric acid and eluted for rubidium and strontium separation on cation exchange columns (BioRad AG 50W-X8 200–400 mesh). Hydrochloric acid (2–2.4 M) is commonly used as an eluent for separation of both of these elements and 2–2.4 M hydrochloric acid elutes potassium and rubidium at the same time (Fig. 2a). For calcium rich samples, the separated rubidium fraction includes much calcium, which disturbs the analyses of rubidium, when loading the rubidium fraction on a filament with phosphoric acid, heating filaments in mass spectrometer and so on. We used both 1.2 M and 2.4 M hydrochloric acid as an eluent for rubidium separation in this study. The optimal results of separation obtained using the combination of 1.2 M and 2.4 M hydrochloric acid are shown in Fig. 2b.

Separated rubidium and strontium fractions were converted to nitrate forms and loaded on a single tantalum filament with 1 μl of 2 M phosphoric acid. Concentrations of rubidium and strontium were determined on spiked fractions with a Finnigan MAT Thermoionic Quadrupole Mass Spectrometer at Nagoya University. The

Table 2. Analytical data of fracture minerals

Sample		Rb (ppm)*	Sr (ppm)*	$^{87}Rb/^{86}Sr$	$^{87}Sr/^{86}Sr$ ($2\sigma_m$)**
#20-1	calcite	0.160	28.8	0.0161	0.704841 (17)
	zeolite	22.0	114	0.558	0.705156 (16)
	bulk	8.42	83.4	0.292	0.704900 (17)
#20-2	calcite	16.9	160	0.304	0.704903 (16)
	epidote	102	866	0.340	0.704980 (14)
	bulk	92.8	862	0.311	0.705001 (16)
#133-all	calcite	0.709	25.0	0.0820	0.704831 (17)
	zeolite	27.5	113	0.703	0.705363 (17)
	bulk	14.5	85.8	0.489	0.705077 (16)
#133-1-1	calcite	0.166	25.9	0.0185	0.704642 (13)
#133-1-2	calcite	0.364	24.8	0.0425	0.704650 (27)
#133-1-3	calcite	0.063	15.4	0.012	0.704683 (16)
#133-1-4	calcite	—	27.6	—	0.704626 (28)
#133-1-5	calcite	0.032	31.8	0.0029	0.704661 (23)
#133-1-6	calcite	0.634	24.5	0.0747	0.704735 (30)
#133-2	calcite	2.11	38.1	0.160	0.704850 (17)
	zeolite	24.9	113	0.635	0.705306 (18)
	bulk	33.0	106	0.902	0.705632 (14)
#153-1	calcite	4.01	66.1	0.175	0.704880 (16)
	zeolite	17.0	88.8	0.554	0.705282 (16)
	bulk	15.2	85.9	0.512	0.705222 (16)
#153-2-all	calcite	2.58	35.5	0.210	0.704856 (17)
	zeolite	15.1	87.6	0.499	0.705131 (16)
	bulk	14.3	86.1	0.480	0.705120 (16)
#153-2-1	calcite	4.78	64.9	0.213	0.705046 (16)
	zeolite	17.9	77.7	0.666	0.705433 (16)
	bulk	18.8	79.5	0.683	0.705470 (16)
#153-2-2	calcite	7.71	88.4	0.252	0.705268 (14)
	zeolite	10.4	56.1	0.538	0.704990 (18)
	bulk	10.3	60.0	0.498	0.705012 (16)
CVS-all	calcite	0.669	181	0.0107	0.704608 (18)
	zeolite	6.54	82.0	0.231	0.704996 (16)
	bulk	3.80	141	0.0777	0.704700 (14)
CVS-1	calcite	0.170	272	0.0018	0.704596 (14)
	zeolite	3.17	205	0.0448	0.704787 (14)
	bulk	1.33	256	0.0151	0.704647 (16)
CVS-2	calcite	0.136	176	0.0022	0.704647 (18)
	zeolite	4.07	591	0.0199	0.704744 (16)
	bulk	0.728	258	0.0082	0.704686 (16)
CVS-3	calcite	0.070	213	0.0009	0.704634 (17)
CVS-4	calcite	0.253	246	0.0030	0.704602 (14)
	zeolite	3.60	338	0.0308	0.704731 (14)
	bulk	8.43	166	0.147	0.704832 (16)

**Analytical errors are within two percents of the abundance values.*
***Errors refer to last two digits and 2 standard errors of the mean of mass spectrometry.*

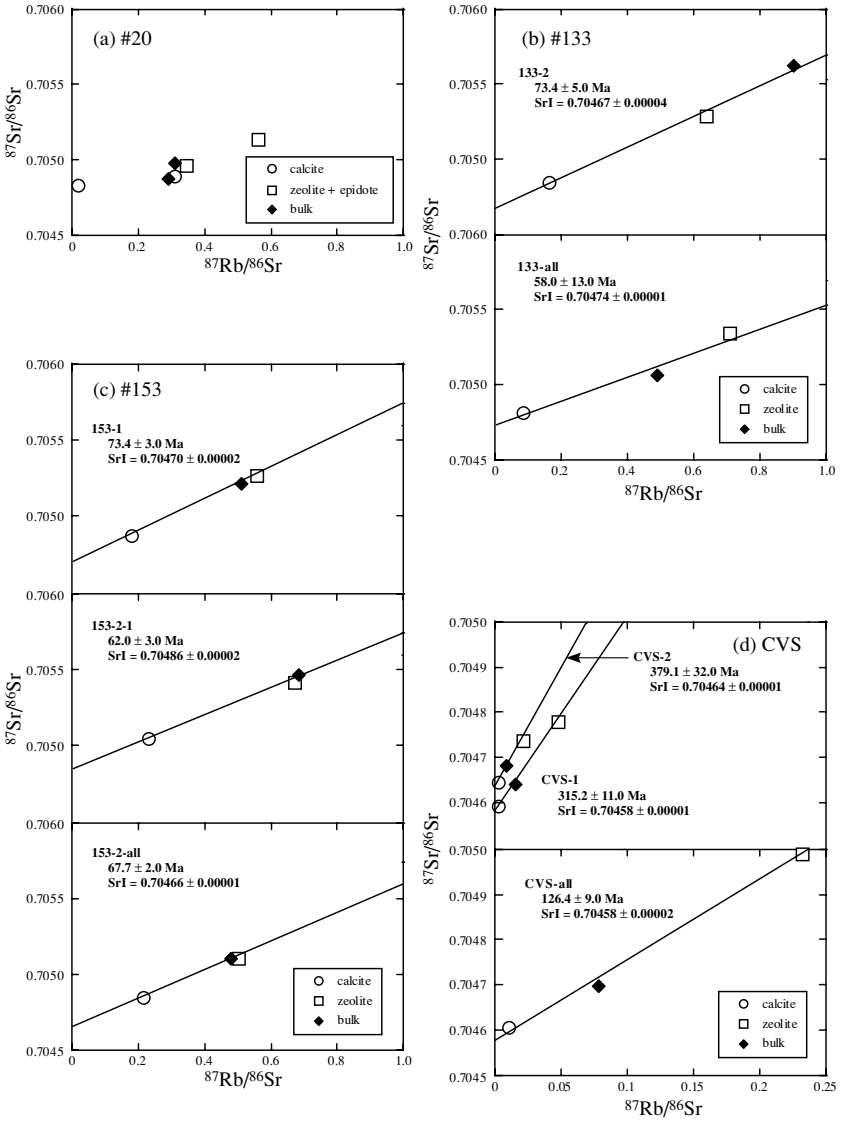

Fig. 3. Rb–Sr isochron plots for each fracture. Open circles represent calcite. Open squares represent zeolite, except for sample #20-2, where it represents epidote. Solid rhombus represent bulk fracture-filling mineral.

ion beams of both elements were maintained at more than 10 mV even in the weakest ion beam currents. Strontium isotope compositions were measured with a VG Sector 54 thermal ionization mass spectrometer in multidynamic mode at Nagoya University. The ^{88}Sr ion beam was maintained at 1.0 V (0.010 nA). $^{87}Sr/^{86}Sr$ isotopic ratios during the measurement were normalized to $^{86}Sr/^{88}Sr$ = 0.1194 by the exponential law. The average $^{87}Sr/^{86}Sr$ ratio of the NIST-SRM 987 strontium standard during the course of this study was 0.710244 ± 0.000021 (2σ, n = 36). Total procedural blanks were 0.4 ng for rubidium and 0.8 ng for strontium. Rubidium blank correction was carried out on all analyses, whereas the strontium blank was considered negligible.

RESULTS

The results are listed in Table 2. Isochrons were not formulated from all analyzed samples (Table 2 and Fig. 3). In particular, none of the samples from location #20 defined an isochron (Fig. 3a). Isochron plots for those of the samples from locations #133, #153 and CVS that were regarded as isochrons and obtained ages are shown in Figs. 3b to 3d. The bulk samples of #133-2 and #153-2-1 do not plot between calcite and zeolite. It is suggested that Rb-rich minerals are unevenly distributed in these samples. The CSV samples were the only ones where a relationship between the distance from the host wall rock and mineral isochron age was evaluated. For these samples,

the isochrons indicate that calculated age decreases with increasing distance from the host wall rock. However, these ages were older than that of skarn formation for reasons described in the discussion. Initial strontium isotopic ratios measured from the fracture-filling minerals were found to be lower than that of recent rainwater at the Kamaishi mine (0.7077; Takagi *et al*., 2001a) and almost identical to those of the present groundwaters in the mine (0.7045 to 0.7048; Takagi *et al*., 2001a). The details of each isochron are described in the following section.

DISCUSSION

The age of fracture-filling minerals in the Kurihashi granodiorite

The age of crystallization of the fracture-filling minerals from groundwater in the Kurihashi granodiorite is estimated to be in the range of 74 to 58 Ma (Figs. 3b and 3c). The main factors contributing to the formation of fractures are igneous activity and subsequent cooling. The Tohoku region experienced violent igneous activity from the Late Cretaceous to the Tertiary. The fractures may have been formed as a result of these activities. Amano *et al*. (1999) and Yoshida *et al*. (2000) reported on the cooling and hydrothermal history of the Kurihashi granodiorite, according to their FT data of fracture-filling apatite and zircon and mineralogical observations. They suggested that the fracture-filling minerals with a high-temperature alteration type were formed at 80–90 Ma when the pluton was cooler than 300°C. They also suggested that the fracture-filling minerals of a low-temperature type were formed after 80 Ma when the pluton was cooler than 200°C. In the low-temperature alteration zone, the ages of fracture formation determined in our study agree well with the conclusions of Amano *et al*. (1999). Therefore, it is considered that these fractures were formed no later than the age obtained by the current Rb–Sr method.

A valid age could not be derived for some samples, even though all samples were analyzed using the same procedure. Rocks in the deeper parts of the Kamaishi mine show evidence of strong geothermal alteration. The sample from location #20 was the deepest sample collected (Fig. 1) and the fracture exhibited a high-temperature alteration zone. Subsequent low-temperature alteration of the fracture-filling minerals after deposition may be the reason that no isochron was defined for this sample location.

Sample #153-2-2 also came from a fracture exhibiting a high-temperature alteration zone. Other samples at the location #153 defined ages. #153-2-2 was closer to the host wall rock than #153-2-1 and might be influenced by the formation of low-temperature type minerals.

Sample #133-1 series contained only calcite. These

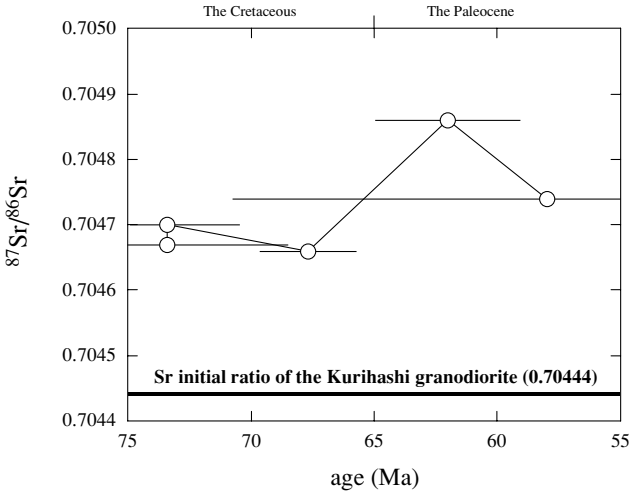

Fig. 4. The transition over time of the $^{87}Sr/^{86}Sr$ isotope ratio of groundwater in the Kamaishi mine. Error bars of the $^{87}Sr/^{86}Sr$ isotopic ratios are smaller than the size of circles. Strontium initial ratio of the Kurihashi Granodiorite (0.70444) is taken from Takagi et al. (2001a).

$^{87}Sr/^{86}Sr$ ratios agree well each other within the range of analytical error. The fracture-filling calcite probably crystallized at the same time. Although rubidium contents of the calcite vary locally (0.03 to 0.7 ppm), the abundances are so low to have any influence on $^{87}Sr/^{86}Sr$ initial ratio in 80 Ma.

The age of fracture-filling minerals in the skarn

The isochrons derived from fracture-filling minerals from the skarn indicate a crystallization age in the range 120 to 380 Ma (Fig. 3d) and show that age decreases with increasing distance from the host wall rock. However, these ages are much older than the latest Cretaceous, when the Ganidake complex intruded and formed the skarn. The age derived for sample CVS-2 (379 Ma) is older than the Late Carboniferous to the Early Permian, when the raw material of this skarn was formed. If the raw material of this skarn was not thermally affected by the intrusion of the Ganidake complex, the fracture ages may suggest the fault ages prior to skarnization.

Ochiai *et al*. (1987) reported that lithophile elements in the limestone and elsewhere in the complex were leached out by hydrothermal waters during skarnization. They also reported that rubidium is more easily removed than strontium during skarnization. Therefore the Rb/Sr ratio may be reduced by skarnization to a level lower than that of the original limestone. The strontium isotopic composition is not significantly reset during skarnization. Therefore, hydrothermal leaching during skarnization may have affected the isochron derived from the skarn samples resulting in erroneous old ages.

Application of Rb–Sr mineral isochron dating to fracture-filling minerals

The previous discussions suggest how to apply Rb–Sr mineral isochron dating to fracture-filling minerals. (1) There must be more than two paragenetic minerals in the fracture. These minerals can be dissolved with different acid reagents (e.g., acetic acid, dilute and cold hydrochloric acid, concentrated and hot hydrochloric acid). In our study, fractures had various minerals including laumontite. As stated previously, laumontite reacts with hydrochloric acid to produce gelatinous material (Murata, 1943) and stilbite cannot be separated from zeolite fraction with hydrochloric acid. (2) The surrounding host wall rocks should not have too much reddish-halo. If the reddish-halo is conspicuous, it is advisable to sample the central part of the fracture would rather be used. In this case, the obtained age is possibly younger than the fracture-filling mineral age obtained from an area which is devoid of a halo. (3) The fracture-filling mineral age in the metamorphic rocks cannot be obtained. In our study, the ages in the skarn was not obtained because of high-temperature alteration. If however the fracture was formed *after* high-temperature alteration, it may be possible to obtain the fracture-filling age.

The transition over time of the $^{87}Sr/^{86}Sr$ isotope ratio of groundwater

We examined the initial $^{87}Sr/^{86}Sr$ ratio for fractures formed in the Kurihashi granodiorite. The initial $^{87}Sr/^{86}Sr$ ratio represents that of the original groundwater from which the fracture-filling minerals were precipitated. The ratio increased to a maximum value of 0.70486 at 62 Ma as shown Fig. 4. There are two possible explanations for fluctuations of $^{87}Sr/^{86}Sr$ ratios in groundwater.

The first is flooding by rainwater. Previous studies have suggested that the $^{87}Sr/^{86}Sr$ ratio of rainwater in coastal areas is very close to that of seawater (e g., Herut *et al*., 1993; Bullen *et al*., 1997; Nakano and Tanaka, 1997). Studies of post-Cretaceous marine carbonates have shown that $^{87}Sr/^{86}Sr$ ratios of seawater have been between 0.707 and 0.709 since the Cretaceous (Burke *et al*., 1982). Because there is no post-Cretaceous marine sedimentary rock which covers the Kamaishi mine, the source of strontium with such a high $^{87}Sr/^{86}Sr$ ratio might suggest that rainwater has soaked directly into the fractures. However, this explanation is inconsistent with the previous study. Present rainwater makes little influence on the present groundwater for its $^{87}Sr/^{86}Sr$ ratio (Takagi *et al*., 2001a).

A second explanation is dissolution of the host wall rock. All rocks react with water although the reaction rate is very slow. A leaching experiment on the Kurihashi granodiorite using distilled water suggested that the $^{87}Sr/^{86}Sr$ ratio of the leachate (0.705 to 0.709) was higher than that of the granodiorite itself (0.705) in the earliest stage of dissolution (Takagi *et al*., 2001b). We cannot preclude the possibility that the cracks were younger in some areas and that water passed through the new cracks brought radiogenic ^{87}Sr which precipitated in carbonate at 64 Ma.

Conclusions

We attempted to determine the age of formation of fractures in the Kamaishi mine by applying the Rb–Sr mineral isochron method to fracture-filling paragenetic calcite and zeolite. In the Kurihashi granodiorite, the age of fracture formation was determined to be in the range 74 to 58 Ma. These ages may represent fracturing during large-scale igneous activity in the Late Cretaceous or during cooling of the granodiorite.

The fracture ages determined from samples taken from the skarn were apparently older than their host wall rocks. This result may have been caused by selective leaching of rubidium during skarnization.

The observed variation of initial $^{87}Sr/^{86}Sr$ ratios with time may be a reflection of underground environmental changes over time.

Acknowledgments—We thank the staff of the Department of Earth and Planetary Sciences, Nagoya University for constructive comments. We would especially like to express our thanks to Dr. Y. Asahara for advice on isotope analysis. We also extend our thanks to Prof. Y. Yusa of Fuji Tokoha University and Dr. K. Aoki and Dr. K. Amano of the Japan Atomic Energy Agency for advice on geology and sampling methods. We thank the administration of the Kamaishi mine for permission to collect samples. We are grateful to Dr. K. Shibata and Dr. H. Kamioka and an anonymous reviewer for their critical and helpful reviews.

References

Amano, K., Ota, K., Yoshida, H. and Semba, T. (1999) Overview of fracture systems in the Kurihashi granodiorite at the Kamaishi Mine. *JNC TN7400 99-007*, 57–65.

Bar, M., Kolodny, Y. and Bentor, Y. K. (1974) Dating faults by fission track dating of epidote—an attempt. *Earth Planet. Sci. Lett.* **22**, 157–162.

Bullen, T., White, A., Blum, A., Harden, J. and Schulz, M. (1997) Chemical weathering of a soil chronosequence on granitoid alluvium: II. Mineralogic and isotopic constraints on the behavior of strontium. *Geochim. Cosmochim. Acta* **61**, 291–306.

Burke, W. H., Denison, R. E., Hetherington, E. A., Koepnick, R. B., Nelson, N. F. and Otto, J. B. (1982) Variation of seawater $^{87}Sr/^{86}Sr$ throughout Phanerozoic time. *Geology* **10**, 516–519.

Cathelineau, M., Fourcade, S., Clauer, N., Buschaert, S., Rousset, D., Boiron, M-C., Meunier, A., Lavastre, V. and Javoy, M. (2004) Dating multistage paleofluid percolations: A K–Ar and $^{18}O/^{16}O$ study of fracture illites from altered

Hercynian plutonites at the basement/cover interface (Poitou High, France). *Geochim. Cosmochim. Acta* **68**, 2529–2542.

Hamabe, S. and Yano, T. (1976) Geological structure of the Kamaishi mining district, Iwate Prefecture, Japan. *Mining Geol.* **26**, 93–104 (in Japanese with English abstract).

Herut, B., Starinsky, A. and Katz, A. (1993) Strontium in rainwater from Israel: Sources, isotopes and chemistry. *Earth Planet. Sci. Lett.* **120**, 77–84.

Hurford, A. J. (1990) Standardization of fission track dating calibration-recommendation by the Fission Track Working Group of the IUGS Subcommission on Geochronology. *Chem. Geol.* **80**, 171–178.

Ikeya, M., Miki, T. and Tanaka, K. (1982) Dating of a fault by electron spin resonance on intrafault materials. *Science* **215**, 1392–1393.

Murata, K. J. (1943) Internal structure of silicate minerals that gelatinize with acid. *Am. Mineral.* **28**, 545–562.

Nakano, T. and Tanaka, T. (1997) Strontium isotope constrains on the seasonal variation of the provenance of the base cations in rain water at Kawakami, central Japan. *Atmos. Environ.* **31**, 4237–4245.

Ochiai, K., Yoshida, T. and Aoki, K. (1987) Mobility of trace elements in the zoned skarns at the Nippo and Shinyama ore deposits, Kamaishi mine. *Res. Rep. Lab. Nucl. Sci. Tohoku Univ.* **20**, 114–130. (in Japanese).

Rousset, D. and Clauer, N. (2003) Discrete clay diagenesis in a very low-permeable sequence constrained by an isotopic (K–Ar and Rb–Sr) study. *Contrib. Mineral. Petrol.* **145**, 182–198.

Shibata, K., Nakajima, T., Sangawa, A., Uchiumi, S. and Aoyama, H. (1989) K–Ar ages of fault gouges from the Medium Tectonic Line in Shikoku. *Bull. Geol. Surv. Japan* **40**, 661–671 (in Japanese with English abstract).

Takagi, M., Tanaka, T., Asahara, Y., Aoki, K. and Amano, K. (2001a) Chemical weathering of rocks in the view of Sr isotopic ratio: Study of groundwater at Kamaishi mine. *Geochemistry* (*Chikyukagaku*) **35**, 61–72 (in Japanese with English abstract).

Takagi, M., Tanaka, T. and Asahara, Y. (2001b) Crystal structure control in elemental dissolution: Evidence from ^{87}Rb–^{87}Sr isotope systematics. *11th Annual V. M. Goldschmidt Conf. Virginia* [CD #3538].

Yoshida, H., Aoki, K., Semba, T., Ota, K., Amano, K., Hama, K., Kawamura, M. and Tsubota, K. (2000) Overview of the stability and barrier functions of the granitic geosphere at the Kamaishi Mine: relevance to radioactive waste disposal in Japan. *Eng. Geol.* **56**, 151–162.